

Student thesis series INES nr 469

Snow insulation effects across the Arctic

Evaluating a revised snow module in LPJ-GUESS

Alexandra Pongracz

2019
Department of
Physical Geography and Ecosystem Science
Lund University
Sölvegatan 12
S-223 62 Lund
Sweden



Alexandra Pongracz (2019).

Snow insulation effects across the Arctic - Evaluating a revised snow module in LPJ-GUESS

Snöisoleringseffekter över Arktis - Utvärdering av en reviderad snömodul i LPJ-GUESS

Master degree thesis, 30 credits in *Geomatics*

Department of Physical Geography and Ecosystem Science, Lund University

Level: Master of Science (MSc)

Course duration: *September* 2018 until *January* 2019

Disclaimer

This document describes work undertaken as part of a program of study at the University of Lund. All views and opinions expressed herein remain the sole responsibility of the author, and do not necessarily represent those of the institute.

Snow insulation effects across the Arctic

Evaluating a revised snow module in LPJ-GUESS

Alexandra Pongracz

Master thesis, 30 credits, in *Geomatics*

Frans-Jan W. Parmentier
Lund University

Paul Miller
Lund University

David Wårlind
Lund University

Exam committee:
Virginia Garcia, Lund University
Dan Metcalfe, Lund University

Abstract

Snow insulation effects across the Arctic

by Alexandra Pongracz

The effect of future changes in temperature and precipitation patterns on arctic ecosystem functioning is often assessed using state-of-the-art ecosystem models. Many models however lack detailed representation of wintertime processes, as pointed out by recent studies (Wang et al., 2016; Slater and Lawrence, 2013). This bias may influence the derived outputs, such as soil temperature, permafrost extent and global carbon budget estimations.

In this project, the dynamic vegetation model LPJ-GUESS was applied with different complexity snow schemes, with the aim of assessing whether the developments in snow dynamics enhance the performance of the model in relation to air-soil temperature relationships (snow insulation effect). We hypothesise that refinement of the snow scheme can provide higher agreement between modelled and observational entities.

The single site analysis showed that a newly developed *Advanced multi-layer*, intermediate complexity scheme is best suited to simulate internal snow dynamics, and the derived snow depth and soil temperature outputs are comparable to measured entities. The regional multi site analysis showed that the *Advanced multi-layer* scheme can best capture the air-soil temperature variability, but the insulation effect is smaller than observed. The effect of using different snow schemes is evident from the simulated Arctic active layer depth and permafrost extent.

Based on these results, the quantification of the snow insulation effect on soil properties and permafrost extent may prompt developments in the model's structural scheme. These updates could help to simulate physical and biogeochemical processes with reduced uncertainty at high latitudes.

Acknowledgements

Firstly, I would like to thank my supervisors Frans-Jan Parmentier, David Wårlind and Paul Miller for their encouragement and constructive suggestions throughout this thesis project. Your advice and support have been a great help in the planning and development of this thesis and I'm looking forward to continuing this project. I would also like to thank the people at INES for their help directly or indirectly to complete this project. Finally, heartfelt thanks go to my family and friends, who supported me during this busy period.

This thesis would not be the same without you!

Contents

Abstract	iv
Contents	vi
1 Introduction	1
1.1 Background	1
1.2 Snow-soil interactions	2
1.3 Ecosystem modelling	4
1.4 Aim	5
2 Materials and Methods	6
2.1 Data	6
2.2 Simulation set-up	7
2.3 Analysis methods	11
3 Results	13
3.1 Single-site analysis	13
3.1.1 Evaluation of the <i>Advanced multi-layer</i> scheme	13
3.1.2 Validation of soil temperature and snow depth	13
3.2 Multi-site analysis	15
3.2.1 Evaluation of air-soil temperature differences	15
3.2.2 Permafrost properties at CALM sites	17
3.2.3 Pan-Arctic permafrost extent	19
4 Discussion	20
4.1 Overall assessment of performance	20
4.2 Sodankylä site simulations	20
4.3 Evaluation of air-soil temperature differences	21
4.4 Evaluation of permafrost dynamics	23
4.5 Shortcomings and future improvements	24
5 Conclusion	25
A Supplementary data	26
List of Figures	28
List of Tables	29
Bibliography	30

1 Introduction

1.1 Background

Since the 1990s, numerous studies have investigated vegetation productivity at high latitudes, and the impact of climatic changes on these ecosystems (Keenan and Riley, 2018). In recent years there has been an increased attention on identifying the drivers of change in this region. The Arctic is expected to be highly susceptible to the climatic changes it will face in the coming years and decades (Meyer et al., 2014).

Recently, the *Snow, Water, Ice and Permafrost in the Arctic (2017)* report assessed the state of the Arctic, potential future changes and their effect on the global scale. The report established that temperature is rising faster at higher latitudes than in other regions. The Arctic is estimated to undergo 4 °C warming of air temperature in the next 30 years and changes in precipitation patterns are also predicted (Christensen et al., 2017). The main question remains how the terrestrial biosphere would react to these proposed changes, in particular the net exchange of carbon with the atmosphere. Due to uncertainties in model projections, it is still unclear whether the Arctic will act as a source or a weak carbon sink in the future (McGuire et al., 2012; Le Quéré et al., 2018).



FIGURE 1.1: The Pan-Arctic study region and estimated permafrost cover by the Circumpolar Active Layer Monitoring program (Brown et al., 2002). Retrieved from <http://www.grida.no/resources/5234>; Accessed 3 January, 2019; Credit: Hugo Ahlenius UNEP/GRID-Arendal.

Carbon dynamics

Permafrost - ground that has a temperature below 0 °C for at least two or more consecutive years - has an important influence on arctic ecosystems, affecting hydrology, soil properties, vegetation composition and distribution. Approximately 25 % of the ice-free land surface of the Northern Hemisphere is underlain by permafrost, adding up to an estimated 16.2×10^6 km² large area (Zhang et al., 2014; McGuire et al., 2018). The assessment prepared by the Permafrost Carbon Network projects a decrease of 1-6 million km² in permafrost area by 2100, the magnitude of which depends on the applied climate scenario (McGuire et al., 2018). This can influence the substantial amount of buried organic C (estimated at 1300 Pg by Peng et al. (2016)) in permafrost soils. Release of greenhouse gases due to thawing permafrost can act as a positive feedback on

climate, and therefore it is important to further evaluate cause and effect relationships across these regions (Koven, Riley, and Stern, 2013).

It is still uncertain how altered climatic patterns will affect permafrost distribution and active layer depths (ALD). Zhang et al. (2014) state that, while on a continental scale permafrost distribution is governed by air temperature, at smaller scales vegetation cover and soil conditions need to be considered. Snow is noted as the most important control on soil temperature at regional scales (Lawrence and Slater, 2010). Soil temperature affects the permafrost covered area, greenhouse gas fluxes and soil carbon stock.

1.2 Snow-soil interactions

Snow provides an insulating cover over the ground, dampening the loss of heat during cold periods (Mackiewicz, 2012). This insulation effect is dependent on a number of factors, such as the length of the snow season and snow depth. The most relevant snow related entities used to estimate snow insulation are listed below. Table 1.1 provides a theoretical range of key variables based on literature sources.

depth (d_s) - Calculated from snow water equivalent (SWE, for instance millimetres of water) and density, that is used as a proxy of the size of the snow pack. SWE is a key variable to keep track of the snow pack's mass and water balance. In short, a thicker snow pack better prevents cooling of the surface, which results in higher underlying soil temperatures.

density (ρ) - Density of snow in a snow pack varies on temporal, as well as at spatial scales. The density of fresh snow is low and increases as snow ages. Denser snow has higher thermal conductivity and thus decreased insulating capacity (Lawrence and Slater, 2010). There are differences in density within the snow pack as well. Density is the primary control on snow thermal properties (conductivity, heat capacity and diffusivity), which can be derived from density using empirical relationships.

thermal conductivity (K_s) - Thermal conductivity is matter's capacity to transfer thermal energy. It is determined by pre-defined, observation-based relationships. In the past 30 years, more than 20 regression relationships were determined and applied in different schemes (Sturm et al., 1997). The question arises: What range is appropriate from a modelling perspective?

volumetric heat capacity (C_s) - Ratio of the energy (heat) added to 1 m³ of matter, resulting in a change of its temperature. It depends on density, just as K_s .

diffusivity (D_s) - Ratio between thermal conductivity and heat capacity. Describes the propagation of temperature through matter (in this case snow or soil layers).

TABLE 1.1: Approximate ranges for key snow variables retrieved from literature sources.

Variable	Range	Unit	Reference
ρ	70-560	kg m ⁻³	Ling and Zhang (2006) and Sturm et al. (1997)
K_s	0.021-0.65	W m ⁻¹ K ⁻¹	Pomeroy and Brun (2001) and Sturm et al. (1997)
C_s	7.5-9 x 10 ⁵	J m ⁻³ K ⁻¹	Ling and Zhang (2006)

These entities are dependent on the composition of the snow pack, namely, the fractions of ice, liquid water and air content. For the sake of simplicity, liquid water content of the snow pack is not represented in this study. In reality, snow density can increase due to a number of different mechanisms - through snow ageing, overburden pressure or destructive metamorphism - and melting-refreezing cycles.

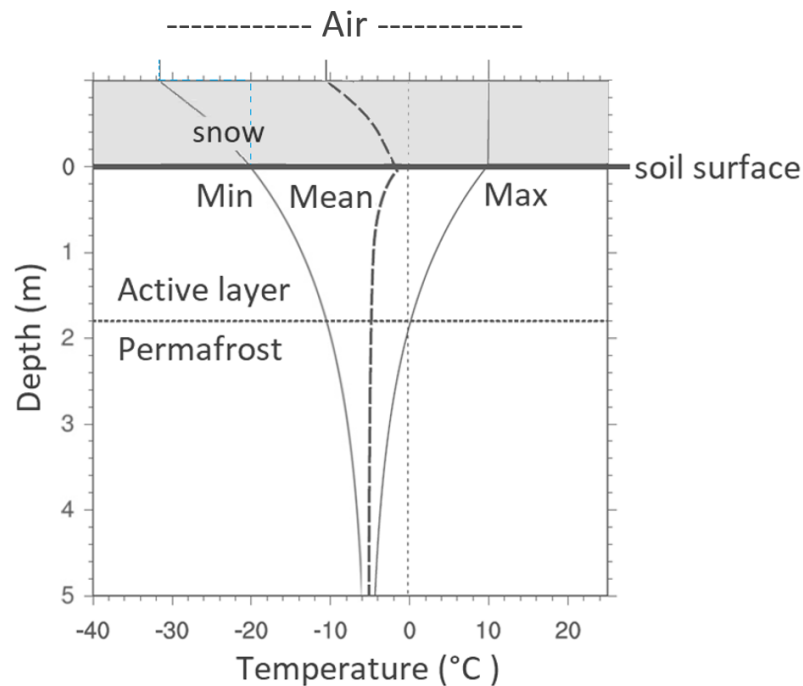


FIGURE 1.2: Theoretical subsurface temperature profile (Koven, Riley, and Stern, 2013). Potential snow cover - shown by the shaded grey area - effectively dampens the cooling effect of air during the cold season. The dashed line shows the average temperature profile; solid lines the seasonal maximum and minimum annual curves.

Figure 1.2 shows the theoretical snow-soil temperature profile for a permafrost underlain area. In permafrost regions, 50-100 % of spatial soil temperature variation can be attributed to changes in snow conditions (Lawrence and Slater, 2010). Soil temperature governs the ALD and permafrost dynamics, and is therefore crucial to take into account. Other aspects to consider are the changes in snow covered area (SCA), directly relating to the albedo feedback. Snow with a high albedo reflects a large portion of the incoming solar radiation, mitigating surface warming. To limit the scope of the study and to be able to attribute divergences in model output variables to structural differences in the applied snow schemes, neither albedo, nor the effects of wind, vegetation cover and composition on snow dynamics are considered in this study. The effects of snow cover changes on surface albedo is not simulated and wind is not included in this model version either. The influence of snow on vegetation is planned to be represented through a cold hardiness sub-model within LPJ-GUESS, but as of now is not treated. As a result, these aspects are not discussed in this project.

CMIP5 (Coupled Model Intercomparison Project Phase 5) climate models project that the winter snowfall rate will increase with a maximum of 45 %, by the year 2100 at high latitudes under a moderate warming scenario, but at the same time the snow season will most likely shorten (Lawrence and Slater, 2010). Collectively, these studies imply that more focus is needed to investigate the dampening effect of snow cover - since the simulated snow dynamics influences

significantly the simulated soil thermal regime and indirectly the computed carbon budget estimates. The relationship with thawing of near surface permafrost is also of interest to be able to thoroughly assess potential changes in the Arctic.

Various projects investigate snow and winter season related processes. The European Space Agency supported GlobSnow project creates spatially large extent, long term datasets of key snow variables (snow depth and snow cover) (Luoju et al., 2011). The Snow Model Intercomparison Project (SnowMIP) highlighted the advances in integrating winter processes, and its importance for the Arctic region (Krinner et al., 2018). These advances prompt development in incorporating snow dynamics in different projection frameworks.

1.3 Ecosystem modelling

A well-established tool is using state-of-the-art, process-based models to simulate potential ecosystem responses to climatic and environmental changes. Models are, by definition, simplifications of reality, and defining the appropriate complexity with which certain processes should be represented is a challenge. This is valid for winter-time processes as well. Abundant available observational data and technical advances promote the evolution of more complex and realistic snow modules. Recently, there has been an increased focus on incorporating these developments in land surface models. Model evaluations regarding snow related processes in global land surface models point to the importance of using a multi-layer snow scheme over a the single-layer scheme (Gouttevin et al., 2012; Krinner et al., 2018).

Recent snow related modelling

Wang et al. (2016) assessed the performance of nine land surface models, in order to reflect on cross-model differences in snow insulation effect in the Northern high latitudes. Their investigation highlighted that there are large deviations between models applying different snow structural representations. They found that models including multiple snow layers and dynamic snow processes performed better compared to other models. The study mentions that besides snow representation, other factors such as soil and vegetation properties and related processes influence the analysed modelled temperature outputs.

LPJ-GUESS

The Lund-Potsdam-Jena General Ecosystem Simulator (LPJ-GUESS) is one of the complex models used to evaluate vegetation responses under different climate scenarios and to determine global carbon budget estimates. The model's performance has been validated both on the regional and the global scale (Zaehle et al., 2014; Smith et al., 2014; Peters et al., 2018).

The simulations provided by models carry a certain uncertainty, and are influenced by the process representations incorporated in the systems. Slater and Lawrence (2013) conclude that certain models have significant snow depth and air temperature biases, stemming from structural representations of cold season processes. Besides affecting soil temperatures, snow changes can also influence carbon stock estimates. Spatially heterogeneous snow thermal conductivity can result in a change in the modelled soil C stocks of 8 % (Gouttevin et al., 2012). The study of Wang et al. (2016) also suggests that model predictions can be adversely affected by a simplistic snow scheme. The snow insulation effect in LPJ-GUESS is smaller than in other models and the difference between air and near surface temperature shows an offset compared to observations.

1.4 Aim

This project sets out to develop the representation of internal snow processes in LPJ-GUESS by adding a new, more complex multi-layer snow scheme. The main aim is to evaluate the model's performance by comparing model simulations to observations, using different complexity snow schemes. In addition, I will assess the potential impact of snow condition changes on soil temperature and permafrost properties across the Arctic.

Approach

The primary model evaluation was implemented through single-site analyses, by assessing the performance of the new, intermediate complexity snow scheme (*Advanced multi-layer* scheme), using customised model simulations driven by observed meteorological data at a Finnish site.

Additionally, to assess the performance of the applied snow schemes, multi-site and regional analyses were used to compare modelled and observed entities using a large set of Russian sites and to assess permafrost active layer depth and spatial extent, compared to previous estimates. We **hypothesise** that improving the currently applied simplistic snow scheme in LPJ-GUESS enhances the accuracy of modelled entities - such as soil temperature - compared to observations. Improving the model will also enable a reassessment of soil-snow-vegetation interactions and their impact on the global carbon cycle.

2 Materials and Methods

For this study, a customised Arctic version of LPJ-GUESS 4.0 (Wania, Ross, and Prentice, 2009; Gerten et al., 2004) was used, with changes to the snow scheme and related modules (LPJ-GUESS SVN Code Repository, revision 7185). LPJ-GUESS uses atmospheric CO₂, precipitation and short-wave (SW) radiation as basic forcing data. In each gridcell, LPJ-GUESS simulates vegetation growth and population dynamics of PFTs (plant functional types) explicitly as a result of growth and competition for resources (Smith, Prentice, and Sykes, 2001). This model includes a complex interaction between processes, including physiological and biogeochemical cycling, plant-soil N-cycling, soil and permafrost dynamics. LPJ-GUESS also has the ability to simulate permafrost (soil thermal) dynamics, which enables us to study soil temperature, ALD and permafrost distribution using this model (Wania, Ross, and Prentice, 2009). For details on model structure, see Smith, Prentice, and Sykes (2001), Smith et al. (2014), Wania, Ross, and Prentice (2009) and references therein.

The spatial extent of this project is limited to the Northern-hemisphere permafrost region. The spatial resolution of simulations is 0.5 x 0.5 degree. Model simulations are initialised with a 500 year long spin-up period - required to initialise potential soil and vegetation conditions - followed by 115 simulation years from 1901 to 2015.

2.1 Data

A summary of used datasets for the model simulations and validation for the project sections are listed in Table 2.1.

Single-site analysis: Sodankylä, Finland

Sodankylä is a site located at lat. 67.37, lon. 26.63 in the Northern boreal region, and is maintained by The Finnish Meteorological Institute - Arctic Space Center (FMI-ARC). This site is marked as an intensive observation area and representative of high latitude ecosystems, thus fitting for our evaluation and validation purposes. The station is on a forest clearing, and the surrounding area consist of forests and some wetlands. The area is characterised by a thin mineral soil, consisting of sand, silt and clay (70, 29 and 1 % respectively) (Essery et al., 2013). Measurements are made in the proximity of trees, but they are not shaded by them, and the measured snow related variables are therefore not biased (Rautiainen et al., 2014). The snow season at the site spans from October to May. The maximum snow depth was 80 cm, and the maximum SWE was 165-240 mm in the period 2009-2012. Sodankylä is characterised by low snow densities and little or no depth hoar formation (Leppänen et al., 2016). This site hosts the so-called *Sodankylä manual snow survey program*, which provides quality checked snow related observational datasets. Data from Sodankylä may be used in upcoming snow model intercomparison projects as reported by Essery et al. (2013). With the aim of testing how the model performs at a single site compared to observed snow dynamics and soil temperature variations, we forced LPJ-GUESS with climatic data collected from Sodankylä. A 7 year long (2007-2014) continuous meteorological dataset of air temperature, short-wave radiation and precipitation was used, provided by FMI. Besides supplying the climatic input for the model, snow depth, air-, snow- and soil temperature measurements at several heights (-80, -40, -20, -10, -5, 0, 10, 20, 30, 40, 50 cm; negative values represent sub-surface, positive values above ground heights) were used to evaluate the model's performance regarding vertical temperature profiles. To align the available observations, the period 2011-2014 was chosen for model validation.

Multi-site analysis

For the multi-site and regional analysis, the CRU-NCEP global reanalysis climate product version 7 - covering the time period 1901-2016 - was used as input for LPJ-GUESS. This is a global gridded atmospheric forcing dataset with $0.5^\circ \times 0.5^\circ$ resolution, including monthly values of air temperature, precipitation and incoming solar radiation. This dataset is commonly applied as an input to land surface models (Viovy, 2016).

Air-soil temperature relationships

The purpose of this regional application is to run LPJ-GUESS with global climatic data and evaluate its performance using a large set of sites with available validation data. Similarly, to the study of Wang et al. (2016), the focus period of this sub-project spans from 1980 to 2000. The model was run for 256 Russian stations, with the aim of comparing observations and simulations of key entities. For this step, quality checked snow depth, monthly near surface air and soil temperature at 25 cm depth data obtained from the Russian Research Institute of Hydrometeorological Information, World Data Center was used (RIHMI-WDC; <http://meteo.ru/>).

Active Layer Depth evaluation

The Circumpolar Active Layer Monitoring (CALM) program, initiated in 1991, sets out to monitor how ALD is affected by climatic changes on long temporal and wide spatial scales. There are more than 200 sites involved and data is made available to the public free of charge. Due to the long measurement period and global extent, a set of 10 CALM sites were chosen for this part of the study (see selected sites in the appendix, Table A.2). These stations have a continuous observational period of more than 10 years, and are spatially representative of the permafrost region.

TABLE 2.1: Input and evaluation data used for this project. Observations are retrieved from: ¹FMI, ²Russian Research Institute of Hydrometeorological Information: World Data Centre, ³CALM Summary Data Table

		Time frame	Simulation forcing	Validation variables
Single site	Sodankylä	2007-2014	precipitation	SWE
			SW radiation	snow depth
Multi site	Russian sites (n=256)	1980-2000	air T ¹	soil T
			CRU-NCEP	air T
	CALM sites (n=10)	1996-2015	precipitation	end of thaw
			SW-radiation	season ALD ³

2.2 Simulation set-up

We tested three set-ups with different complexities of snow representation in LPJ-GUESS - the details of each scenario is shown below and summarised in Table 2.3. Table 2.2 describes the variables used in this project.

TABLE 2.2: Description of key snow variables.

Variable	Description	Unit	Equation
ρ_k	layer density	kg m^{-3}	2.1, 2.2, 2.3, 2.5, 2.6
ρ_0	reference density	kg m^{-3}	2.5, 2.6
g	gravitational constant	m s^2	2.5
M_k	mass above the middle of the snow layer	kg	2.5
η_k	compactive viscosity	Pa s	2.5
T_m	reference temperature	$^{\circ}\text{C}$	2.5
T_k	layer temperature	$^{\circ}\text{C}$	2.5
T_{snow}	snow threshold temperature	$^{\circ}\text{C}$	2.7
$melt$	daily melt water	mm day^{-1}	2.7
t	time step	day	2.5, 2.8
z	layer thickness	m	2.8
D	diffusivity	$\text{W J}^{-1} \text{m}^{-2}$	2.8

Static scheme

Simplistic version as used in the model intercomparison project by Wang et al. (2016). The snow pack is not divided into layers. Compaction is not considered, snow density and thermal properties are set as constants, following literature recommended values (362 kg m^{-3} and $0.196 \text{ W m}^{-1} \text{ K}^{-1}$ respectively).

Simple multi-layer scheme

Basic multi-layer snow scheme. Snow layers are defined daily, based on the size of the snow pack (total SWE) and the user defined maximum layer thickness (50 mm), without preserving information of the potential snow layer distribution from the previous day. Snow density varies between 150 and 500 kg m^{-3} , according to a simple compaction scheme based on snow ageing following Wania, Ross, and Prentice (2009) as expressed in Eq. 2.1:

$$\rho_k = \begin{cases} \rho_{min} & S_{current} \leq 0.75 * S_{prev} \\ \rho_{min} + (\rho_{max} - \rho_{min}) \frac{S_{current} - 0.75 * S_{prev}}{0.25 * S_{prev}} & 0.75 * S_{prev} < S_{current} \leq S_{prev} \\ \rho_{max} & S_{current} > S_{prev} \end{cases} \quad (2.1)$$

Fresh snow density (ρ_{min}) is assumed until the current year's number of snow days ($S_{current}$) reaches 75% of the previous year's total number of snow days (S_{prev}). Afterwards, snow density evolves following Eq. 2.1. This means that compaction only occurs at the last fourth of the snow season and that the updated density is confined between the defined range (ρ_{min} and ρ_{max}). Even though the snow pack is divided into sub-layers (maximum of 5), the layers do not have individual properties, such as density and thermal conductivity and heat capacity. This results from the fact that the layers are defined each day, without taking into account the layer distribution of the previous day. Using the snow ageing scheme, the *Simple multi-layer* set-up preserves constant (low density, freshly fallen snow) snow layer density for all defined layers in the first 75% of the current snow season - behaving much like the *Static* scheme. During the latter quarter of the snow season the snow pack's density (each layer having the same density) will increase daily, following Eq. 2.1. Thermal conductivity (K_s) is dependent on the the layer's calculated density, based on Ling and Zhang (2006), as shown in Eq. 2.2.

$$K_s = 0.138 - \frac{1.01\rho_k}{1000} + 3.233 \left(\frac{\rho_k}{1000} \right)^2 \quad (2.2)$$

Heat capacity (C_s) is calculated using Eq. 2.3, following Ling and Zhang (2006), using air temperature (T_{air}) and snow layer density:

$$C_s = 1000\rho_k(0.185 + 0.00689T_{air}); \quad (2.3)$$

Both in the *Static* scheme and in the *Simple multi-layer* scheme, density is assumed to be equal to ice density in the heat capacity calculation (917 kg m^{-3}). Since this value is almost twice the potential snow density, the derived heat capacity values is approximately 1.9×10^6 . These values are higher than the literature suggested guidelines. Snow layer diffusivity (D_s) is computed as the ratio between thermal conductivity and heat capacity as shown in Eq. 2.4:

$$D_s = \frac{K_s}{C_s} \quad (2.4)$$

Advanced multi-layer scheme

This intermediate complexity multi-layer snow scheme is the most advanced scheme tested and it was incorporated in LPJ-GUESS in this project. Snow layers are defined using the pre-set maximum layer threshold (50 mm), but opposed to the *Simple multi-layer* scheme, the layers are handled dynamically, preserving the layers distribution and properties from the previous day. The *Advanced multi-layer* scheme applies mechanical compaction (Eq. 2.5), based on Best et al. (2011):

$$\frac{\partial\rho_k}{\partial t} = \frac{\rho_k g M_k}{\eta_k} \exp\left(\frac{k_s}{T_m} - \frac{k_s}{T_k} - \frac{\rho_k}{\rho_0}\right) \quad (2.5)$$

The increase in the snow layer's density ($\partial\rho_k$) depends on the mass of overlying layers (M_k). The calculated snow density is confined between 150 and 500 kg m^{-3} . T_m denotes the melting point of water and η_k the compactive viscosity factor (see Table 2.2). k_s is an empirical constant defined by Best et al., 2011, with a value of 4000 K. The snow layers are dynamically handled, using precipitation and air temperature as forcing. If a layer's thickness exceeds a prescribed threshold, a new layer is initiated. If all the layers reach the pre-defined maximum layer depth (50 mm in this case), excess snow is transferred to the bottom layer. This way, the topmost layer is always the thinnest. After snow melt occurs, the layers are reviewed, and snow is redistributed between the existing layers, to ensure realistic snow pack dynamics. Each layer has its own thickness (depth, d_k), mass, density, temperature and thermal properties. K_s in this set up is calculated using a power function on layer density and a reference density (ρ_0) (Eq. 2.6, following (Best et al., 2011)).

$$K_s = 2.22 \left(\frac{\rho_k}{\rho_0} \right)^{1.88} \quad (2.6)$$

Melting, computed by Choudhury and DiGirolamo (1998) (Eq. 2.7) occurs if the temperature of a layer (T_k) is above 0°C , and melt water directly runs to the soil. Each applied snow scheme uses Eq. 2.7 for calculating the amount of daily melt water in the existing layers, where T_{snow} expresses the set threshold temperature for snowfall (0°C in this case).

$$melt = (1.5 + 0.007 * precipitation)(T_k - T_{snow}) \quad (2.7)$$

Each existing layer participates in the compaction process. The increase in layer density due to overburden pressure is dependent on half of the mass of the current layer and the mass of the

overlying snow cover. The resulting pack's density is weighed by the amount of old and new snow present, each day when new snow comes on top of an already existing layer.

Soil and snow layer temperatures are computed taking into account each layer's diffusivity (D) and height (z), using the Crank-Nicholson finite difference method (Eq. 2.8).

$$\frac{\partial T}{\partial t} = \frac{\partial}{\partial z} \left(D(z) \frac{\partial T}{\partial z} \right) \quad (2.8)$$

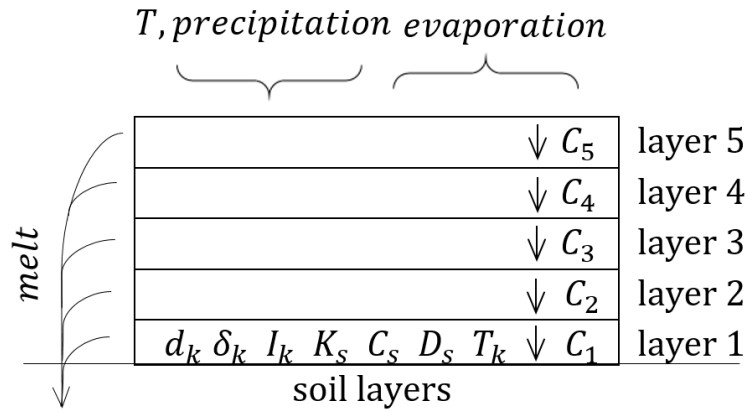


FIGURE 2.1: Snow pack design of the *Advanced multi-layer* scheme (C_1 - C_5 denotes the compaction in each layer).

Figure 2.1 provides a sketch of the updated multi-layer snow pack design. The work-flow of the *Advanced multi-layer* scheme is presented in Figure 2.2. The snow related processes are handled in five major stages. In contrast to previous model versions, each layer has individual physical and thermal properties which are forwarded to the soil-snow temperature calculation function.

The multi-layer approach enables the simulation of thermal gradients inside the snow pack. However, there is no separation between ice and liquid water fractions in the snow layers. Since snow density governs the thermal properties in all applied schemes, we assume that assigning values for each perspective layer and applying a mass-based mechanic compaction scheme will provide a more realistic simulation of the snow profile and the snow pack's internal dynamics. Table 2.3 summarises the structure of the applied snow schemes, based on their key characteristics.

A dynamic and individual representation of snow layers make it possible to save layer specific model outputs, such as density. This way, unlike other models, - such as the model CLM 4.5 (Oleson, Lawrence, and Bonan, 2013) - snow depth is calculated from snow water equivalent based on the simulated daily layer densities, instead of an assumed average density value.

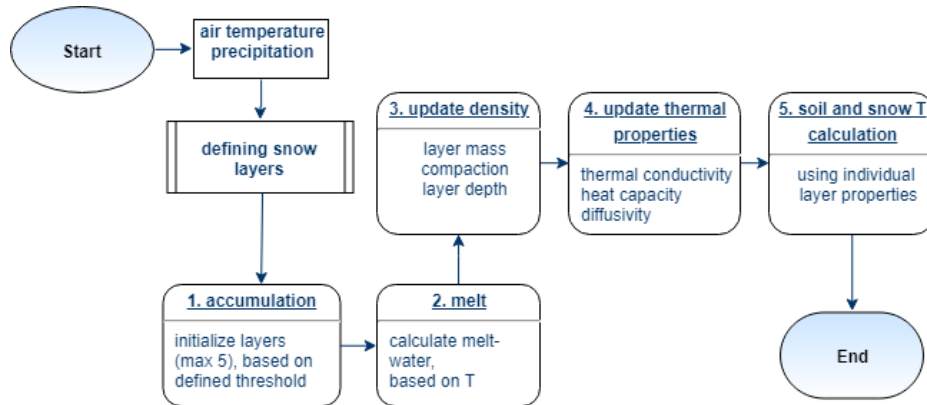
FIGURE 2.2: Work-flow of the updates in the *Advanced multi-layer* scheme.

TABLE 2.3: Characteristics of the applied schemes.

¹Wania, Ross, and Prentice (2009), ²Best et al. (2011), ³Ling and Zhang (2006)

	Static	Simple multi-layer	Advanced multi-layer
Snow layers	static 1 layer	dynamic 5 layers	dynamic 5 layers
Compaction	fixed density	snow ageing ¹ Eq. 2.1	mechanical ² Eq. 2.5
Thermal conductivity	fixed	linear ³ Eq. 2.2	power on density ² Eq. 2.6
Heat capacity	fixed	density based ³ Eq. 2.3	
Water phases	ice only		

2.3 Analysis methods

Firstly, we conducted a single-site (local) analysis, in order to ensure that all integrated snow schemes are functional and to evaluate if the modelled snow and soil temperature dynamics are comparable to site measurements. We extended the area covered by simulations as a next stage, since LPJ-GUESS is calibrated for regional rather than local scale analysis. The Russian sites' analysis made it possible to replicate a methodology applied for the recent study of snow insulation by Wang et al. (2016) and to make use of a large areal cover observation dataset of soil temperature and snow depth variables for validation. The Pan-Arctic simulations were conducted with a diagnostic purpose, visually interpreting the modelled permafrost distribution. The main aim of this latter step was to assess whether the differences in snow depth and soil temperature variables using the three snow schemes for the small scale simulations are shown at a broad scale.

Single-site analysis

For the single-site investigation, LPJ-GUESS was run with observed climatic data for the Sodankylä site (see Table 2.1).

Diagnostics of the new scheme

To evaluate the updates in snow representation in the *Advanced multi-layer* scheme, individual snow layer properties, soil and snow temperature outputs were compared to literature references and observational data. This step was necessary to test if the model is able to simulate realistic

conditions and to ensure it can be used for further analysis. Differences in snow representation within the three snow schemes (*Static*, *Simple*- and *Advanced multi-layer* schemes) are discussed in the corresponding Results section (3.1.1).

Comparison to observations

To study the correspondence between simulated and modelled entities, snow depth and vertical temperature profiles were investigated in the period between October 2007 and October 2014. It is not possible to simulate coinciding rain and snow events by the model, therefore it is necessary to set a threshold temperature to determine when snow fall occurs. Essery et al. (2016) established that the possibility of snowfall is high around 0 °C, and preliminary simulations showed an improved fit when adjusting this temperature threshold to 2 °C. Thus, to account for site specific properties, the temperature threshold in the model below which snow falls was adjusted from the default 0 to 2 °C for all three applied schemes. Since Sodankylä experiences low snow densities (Rautiainen et al., 2014), the density range governing the mechanical compaction in the *Advanced multi-layer* scheme was modified to 100-350 kg m⁻³ and the compaction rate lowered (to 20 % of the default set-up) for the *Advanced multi-layer* scheme. The constant density of the *Static* scheme was defined as 200 kg m⁻³, taking into account the average snow density at the site reported by Rautiainen et al. (2014), based on observations. The preliminary analysis showed that these alterations increased the agreement between observed and estimated entities. These optimisations made possible to relate/appoint differences in the schemes' performance to structural differences, rather than parameter uncertainties.

Multi-site and regional analysis

Air-soil temperature differences

The method used in Wang et al. (2016) was followed to determine whether the higher complexity snow scheme provided a better fit to observations. We assessed the modelled air-soil (25 cm depth) temperature relationship at the same set of Russian sites as in Wang et al. (2016). For this task, the winter months (December-January-February) were used (DJF), between 1980 and 2000. The emphasis was on inspecting the air-soil temperature and soil temperature-snow depth relationships.

Trend in ALD and spatial permafrost extent

Observed end of thaw season ALD between 1996-2015 was compared to simulated maximum ALD at each site. Trends in ALD evolution were assessed and results compared with literature references (such as Luo et al. (2016)). A Pan-Arctic wide spatial analysis was conducted to assess modelled permafrost extent over the study region. Thaw depth is defined in the model as the 0 °C isotherm in the soil, which means that the maximum ALD was derived from the simulations based on the modelled soil temperature. In this study, near-surface permafrost was defined as areas where the maximum ALD was less than 150 cm. Due to time constraints, the areal permafrost cover was compared only qualitatively to the map of Brown et al. (2002) and other modelling studies (McGuire et al., 2018; Koven, Riley, and Stern, 2013).

3 Results

3.1 Single-site analysis

3.1.1 Evaluation of the *Advanced multi-layer* scheme

The seasonality of snow cover and the SWE of each layer is shown in Figure 3.1 a. Since this figure summarises the snow layer characteristics averaged over all simulation years, the fourth layer is only visible in March-May. Due to the low SWE at this site, the potential fifth layer is not simulated.

Figure 3.1 b shows the structure and dynamics of the snow pack from September 1974 to May 1975. It indicates that Layer 1 (bottom layer) is the deepest layer and its height decreases after mid-December, due to compaction and potentially melting. This simulated density pattern within the snow pack - lower layers having higher density and top layers lower density - is consistent with the snow pack characteristics reported from the same site by Esery et al. (2016). The differences in simulated snow cover for the different complexity snow schemes can be seen in Figure A.1. The differences in patterns suggest that indeed the complexity of snow representation influence significantly snow cover dynamics.

3.1.2 Validation of soil temperature and snow depth

Figure 3.2 compares the simulated and observed snow depths throughout seven snow seasons between November 2007 and 2014. As a result of the site specific optimisation, all schemes show skill to approximate snow depth dynamics at Sodankylä. Figure 3.2 a shows that the *Static* scheme generally overestimates the snow depth, except for 2010, when all schemes show larger deviations from the observations. The *Simple multi-layer* scheme provides a good fit in certain years - such as 2011 - but overestimates snow height at the beginning of the snow season in all years - except 2010. The *Advanced multi-layer* scheme seems to consistently underestimate the maximum snow height by 10-15 cm, but follows the seasonal trend of measurements well. Figure 3.2 b confirms the skill of the *Advanced multi-layer* scheme in capturing snow depth dynamics correctly. The scatter of *Simple multi-layer*'s points suggests that this scheme cannot capture snow height dynamics with high precision. The coefficient of determination (R^2) is 0.84, 0.71 and 0.88 for the *Static*, *Simple*- and *Advanced multi-layer* schemes respectively. The RMSE applying the three schemes is 12.41, 15.45 and 10.7 cm, respectively (see

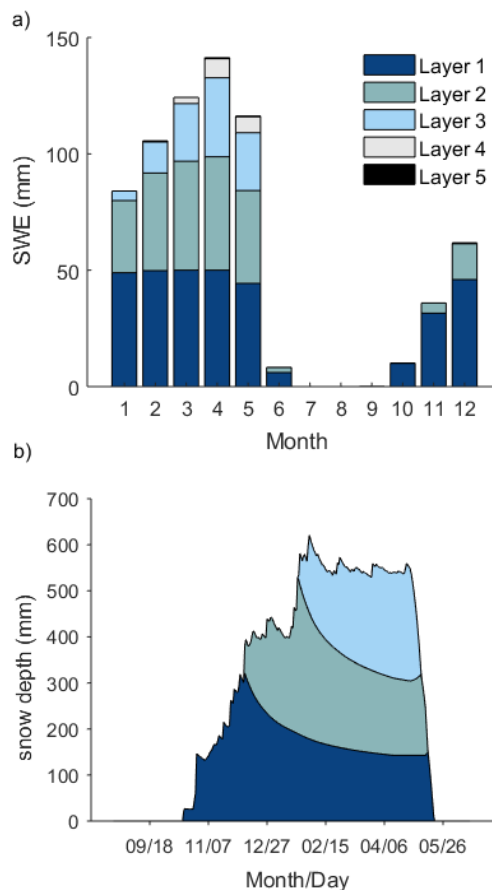


FIGURE 3.1: Average snow layer properties in Sodankylä, applying the *Advanced multi-layer* snow scheme. Colours denote the different snow layers. a) Snow layer division and layer snow water equivalent (SWE) averages per month. b) Simulated snow pack structure at Sodankylä, during a selected snow season.

Appendix Table A.1). The highest calculated R^2 and the lowest RMSE for the *Advanced multi-layer* scheme suggest that the agreement between observed and modelled entities is highest for the *Advanced multi-layer* set up.

Simulated snow depth controls the insulation capacity of snow, and therefore influences modelled soil temperatures directly. To evaluate the differences in snow insulation effect of the new scheme, the simulated soil temperature profiles were compared (Figure 3.3). In general, we can clearly distinguish the different schemes' temperature profiles from one another, which suggests that the complexity and structural representation of snow cover have a significant influence on near surface soil temperatures. This finding aligns with recent modelling studies (Best et al., 2011; Gouttevin et al., 2012; Essery et al., 2013).

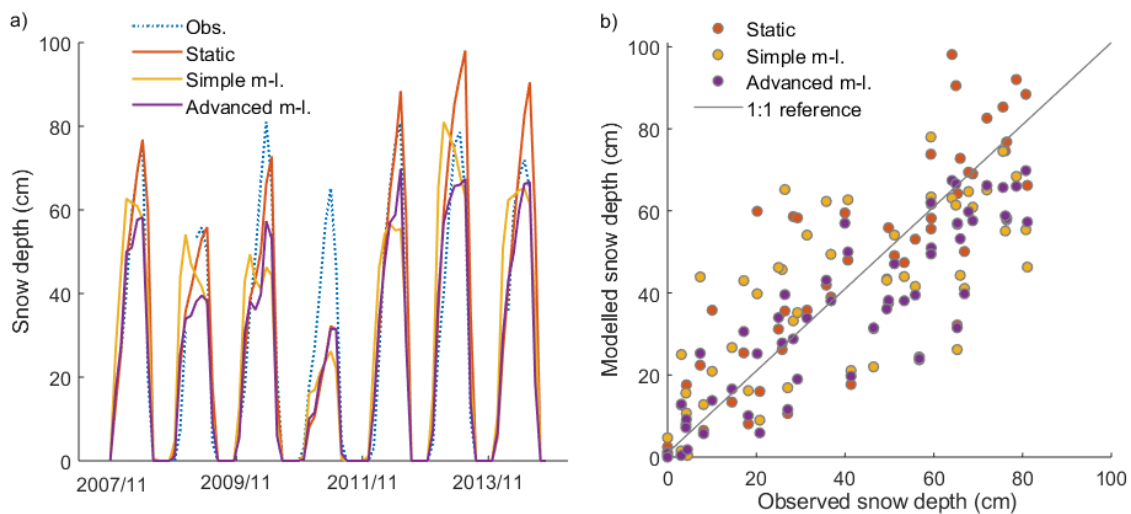


FIGURE 3.2: a) Observed and simulated snow depth at Sodankylä, 2007/11 to 2014/7. Continuous lines represent different model set-ups, the dashed line observed snow height. b) Observed and measured snow depth relationship at Sodankylä (2007-2014). Colours represent different model set-ups.

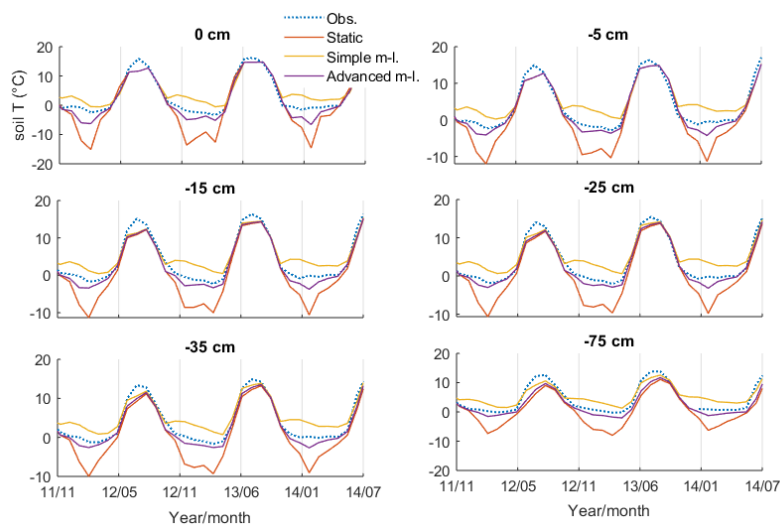


FIGURE 3.3: Observed and modelled soil temperature at six depths, between 2011/11 and 2014/7.

TABLE 3.1: Soil temperature R^2 for the three snow schemes at Sodankylä (2011-2014).

	0 cm	-5 cm	-15 cm	-25 cm	-35 cm	-75 cm
Static	0.84	0.89	0.9	0.9	0.9	0.86
Simple multi-layer	0.95	0.95	0.94	0.94	0.95	0.94
Advanced multi-layer	0.95	0.96	0.97	0.97	0.92	0.95

TABLE 3.2: Soil temperature RMSE ($^{\circ}\text{C}$) for the three snow schemes at Sodankylä (2011-2014)

	0 cm	-5 cm	-15 cm	-25 cm	-35 cm	-75 cm
Static	5.34	4.28	4.35	4.06	4.11	4.5
Simple multi-layer	2.56	2.83	2.51	2.6	2.41	2.21
Advanced multi-layer	2.16	1.58	1.63	1.35	1.43	2.13

Soil temperature observations were available from 2011 onward, thus the sub-surface temperature analysis focuses on this period. All schemes capture spring and autumn temperatures accurately. The *Static* scheme consistently underestimates soil temperatures at all depths during the cold season. On the other hand, the *Simple multi-layer* scheme simulates higher than measured winter temperatures during the study period. The *Advanced multi-layer* scheme has a small negative bias of soil temperature compared to observations, for all investigated layers.

Computed R^2 and RMSE between measured and simulated soil temperatures (presented in Table 3.1 and Table 3.2 indicate the highest agreement applying the *Advanced multi-layer* scheme at all depths.

An interesting feature on Figure 3.3 is that there is a slight difference between measured and simulated soil temperatures at the summer peak, which suggests that the summertime soil thermal properties are not accurate.

3.2 Multi-site analysis

3.2.1 Evaluation of air-soil temperature differences

To quantify and evaluate the snow insulation effect in LPJ-GUESS, the simulations were conducted on a set of 256 Russian sites, as used in (Wang et al., 2016).

Air-Soil temperature & snow depth relationship

The difference between air and soil temperature, ΔT , is used as a proxy for measuring insulation capacity of snow. ΔT relationships for different snow regimes can be seen on Figure 3.4 a. Three temperature classes were defined to assess how snow influences the air-soil temperature relationship during cold, intermediate and warmer air temperature periods. Air temperature can affect snow internal processes, and it is therefore an important factor to account for.

According to observations, the insulation capacity is increasing with snow depth, and shows an asymptotic trend. Snow during warm air temperature conditions (-5 to -15 $^{\circ}\text{C}$) has lowest ΔT values, while the insulation capacity is at its maximum during the coldest conditions. At low ΔT values, the three analysed temperature regimes show a more similar behaviour in the simulations, while at higher temperature differences the three series are easily distinguishable. Except for the *Static* scheme, the other set-up can reproduce the increasing insulation capacity at higher snow depths. The magnitude of ΔT is smaller for the *Advanced* scheme, and higher for the *Simple*

multi-layer scheme compared to observations. It stands out that the *Static* scheme shows a significantly different pattern than both the observations, other schemes, and the results of Wang et al. (2016). A plausible cause of the deviation between the published and current results may be the fact that the Wang et al. (2016) article used another climate dataset (CRU TS30, Harris et al., 2014), compared to the more recent CRU-NCEP version 7 dataset applied in this study.

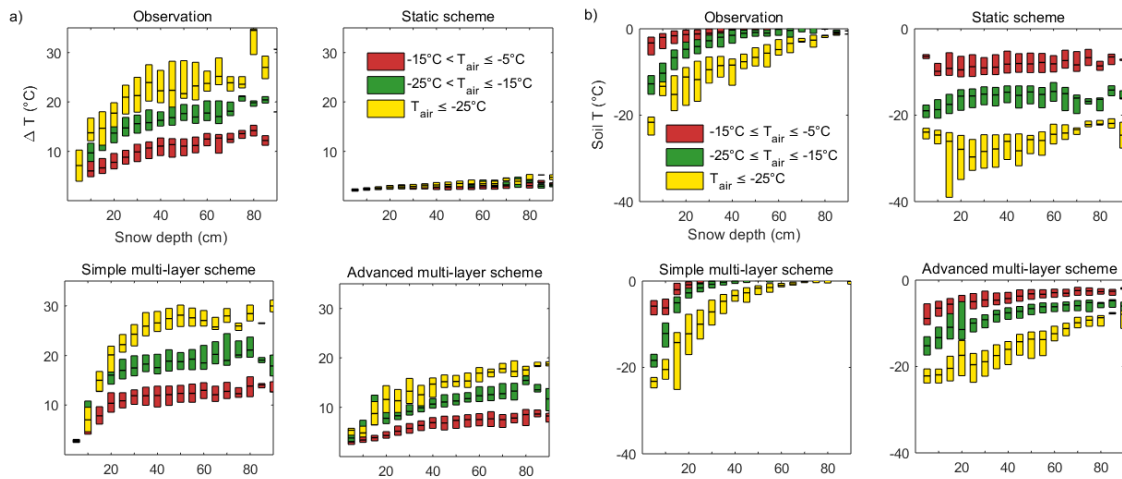


FIGURE 3.4: Snow insulation effect 1980-2000, DJF, observations and model simulations using three snow schemes. Snow depth presented on the horizontal axis is classified in 5 cm depth bins. Colours indicate different air temperature regimes. Upper and lower bars present the 25th and 75th percentiles. a). Difference in air-soil temperature and snow depth relationship. b). Soil temperature and snow depth relationship.

Soil temperature & snow depth relationship

Previous studies confirm the insulating effect of snow depth up to a certain point. This threshold is called the effective snow depth, which can vary depending on site location between approximately 25-40 cm snow height (Slater, Lawrence, and Koven, 2017; Wang et al., 2016). The effective snow depth threshold can be seen from the observational soil-snow relationship on Figure 3.4 b). The *Static* scheme can reproduce neither the range nor the trend of the soil-snow relationship. The *Simple-* and *Advanced multi-layer* schemes can adequately simulate the range of soil temperatures, with the *Advanced multi-layer* scheme showing lower soil temperatures than observed, a behaviour also observed at the single site simulations (Figure 3.3). On the other hand, the *Simple multi-layer* scheme levels off at lower snow depth, than indicated by the measurements.

Bias analysis

Wang et al. (2016) ascertained that the CRU-NCEP version 4 - covering the time period 1901-2008 - climate forcing has a 4.7 °C negative air temperature bias compared to the observations from the set of Russian sites. To test how the meteorological driving data affects the derived outputs, we conducted a sensitivity like analysis by increasing air temperature with 4.7 °C (the bias reported by Wang et al. (2016)). Figure A.2 displays the results of the test simulation for the *Advanced multi-layer* scheme. The ΔT range is higher than with the default simulations, better resembling the measurements. Soil temperature shows a steeper increase at low snow depth, and the shape of the curve compares to the observed relationship. Since the current CRU NCEP driving data is an updated version of the one used in Wang et al. (2016), we additionally calculated the air temperature statistics regarding our applied climate dataset. The RMSE is 1.4 °C and the

model bias compared to observations is $-0.4\text{ }^{\circ}\text{C}$, both of which are smaller deviations from the measurements than in the previous NCEP product.

3.2.2 Permafrost properties at CALM sites

Trends in maximum ALD

To assess the model's ability to capture observed trends in ALD, the statistical characteristics of each CALM study site was computed, which is presented in Table 3.3. The sites are distributed across the Arctic and the ALD measurements are made using different methods (thaw tubes, probing and ground temperature measurements). Besides the different methodology, the spatial resolution of observations also differs. The comparison between modelled and simulated values is thus challenging. It is clear from this table that regarding the 20-year average maximum ALD values the three model schemes show deviations from the observed mean values.

TABLE 3.3: Average annual maximum ALD of selected CALM sites (1996-2015).

Site name	Site code	Observed ALD (cm)	Modelled ALD (cm)		
			Static	Simple m-l.	Advanced m-l.
Barrow	U2	35.9	61.5	66	60.5
Deadhorse	U6	64.8	118.1	122	121
Pearl Creek	U19	70.3	150	150	150
Zackenbergl	G2	64	37	40.5	37.9
Abisko	S2	72	78.6	150	108.5
Vaskiny Dachy	R5	80.2	93.8	128	91.9
Lake Glukhoe	R19	87	98.4	129	117.9
Bykovsky	R29A	84.6	93.1	115.4	94.6
Ayach-Yakha	R2	33	133.5	150	149.3
Reindeer Depot	C7A	134.8	148.9	148.9	129.3

The observed end of season ALD and simulated maximum ALD when applying the different snow schemes can be seen on Figure 3.5. In this project, permafrost was defined having ALD $< 150\text{ cm}$, therefore at the sites where the modelled ALD reaches this threshold - such as U19 and S2- we can conclude that the model does not simulate permafrost conditions. There are big differences in model performance at the sites. In general, the *Simple multi-layer* scheme is predicting the deepest active layer, and the *Static* scheme the shallowest. The *Advanced multi-layer* scheme provides a close fit to the observations at sites R5 and C7A. At other sites - such as U6 and R29A - the model detects the trend, but overestimates ALD. Given that these simulations were run with global and not site specific climate data, soil conditions and that the measurements represent conditions at a constrained locations, evaluating the model performance quantitatively is challenging. Hence, the focus in evaluation is more qualitative and focuses on determining if the model version has the skill to reproduce trends in ALD, and not the absolute accuracy of outputs.

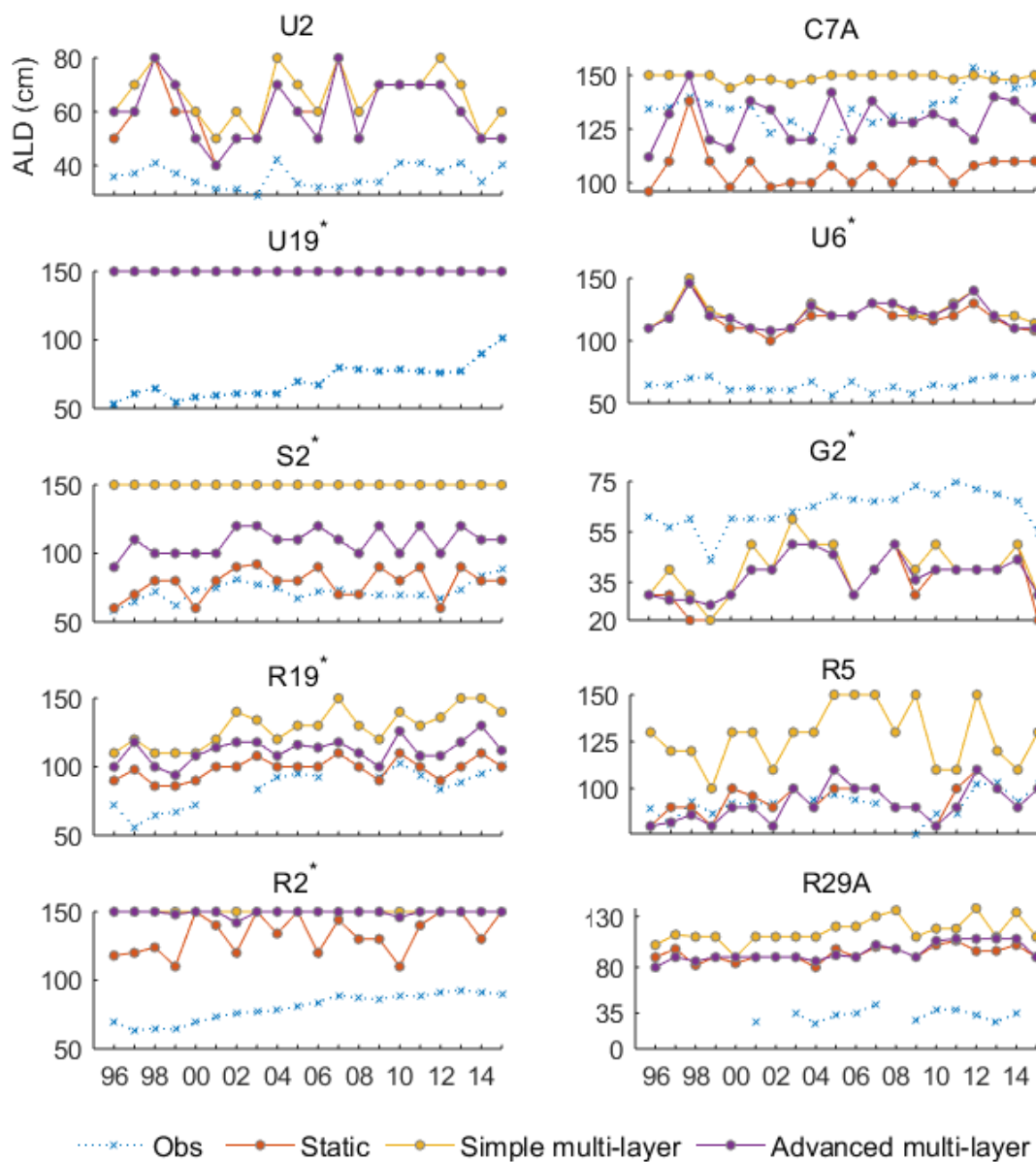


FIGURE 3.5: Maximum seasonal ALD for 10 CALM sites, observations and model simulations, applying three different snow schemes. Sites with a * are marked by Luo et al. (2016) having significant observational trends in ALD.

3.2.3 Pan-Arctic permafrost extent

Large scale ALD patterns were observed by conducting Pan-Arctic simulations while applying each of the three snow schemes. This analysis step had a qualitative focus, aiming at inspecting whether the single-site and multi-site simulation findings hold for the whole Pan-Arctic. The modelled ALD and winter time (DJF average) soil temperature at 25 cm depth is shown on Figure 3.6.

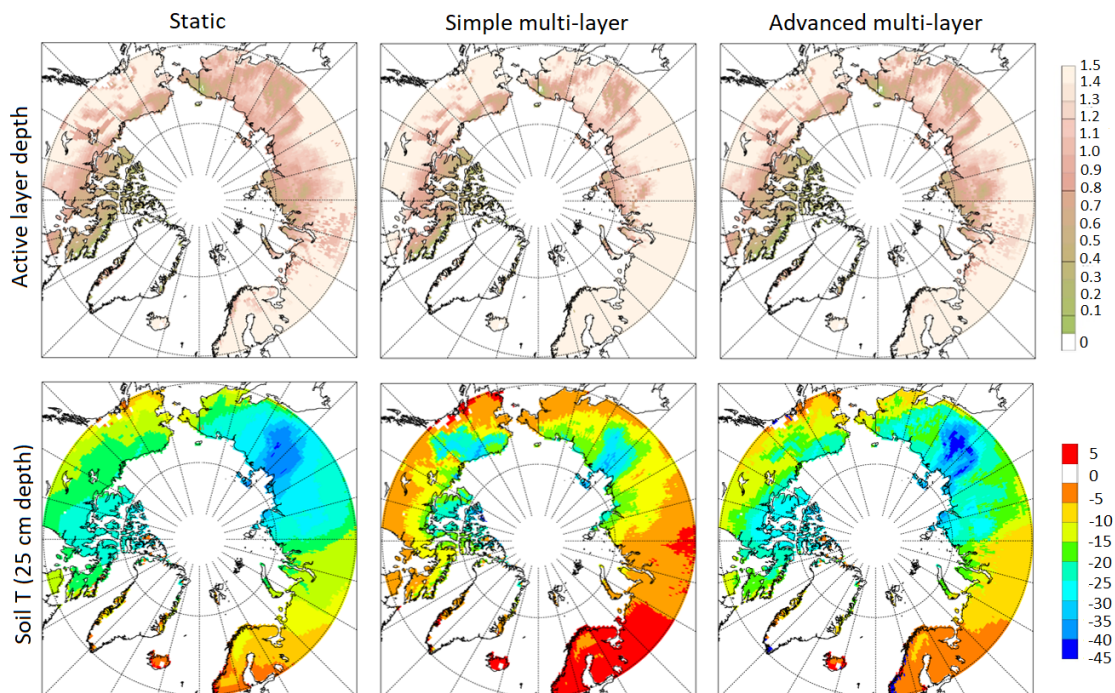


FIGURE 3.6: Pan-Arctic simulations applying the three tested snow schemes, average 1996-2015. Top row: Maximum ALD (in meters), Bottom row: Average winter (DJF) soil temperature at 25 cm depth (in °C).

The permafrost covered area (ALD < 1.5 m) is the smallest using the *Simple multi-layer* scheme, which aligns with the previous findings in Figure 3.3 and 3.4, which show that this scheme simulates a higher than measured insulation effect and increased soil temperatures. The calculated modelled permafrost covered area for the is $11.87 \times 10^6 \text{ km}^2$, $8.351 \times 10^6 \text{ km}^2$ and $10.77 \times 10^6 \text{ km}^2$ for the *Static*, *Simple multi-layer* and *Advanced multi-layer* schemes respectively. The *Static* and *Advanced multi-layer* schemes' permafrost extent is similar to each other, the *Static* one has a shallower ALD in Eastern Russia. Although permafrost areal cover estimates show a large spread, the estimates of these two set ups correspond to the approximate range reported by McGuire et al., 2018; Koven, Riley, and Stern, 2013. The shallow soil temperature figures at the bottom row of Figure 3.6 explains the noted patterns in ALD. The *Simple multi-layer* scheme simulates significantly higher winter soil temperatures across the Arctic region, red and consequently the computed permafrost extent is lower than for the other schemes. The *Advanced multi-layer* scheme shows higher soil temperature values in Northern Europe and Northernmost parts of America.

4 Discussion

4.1 Overall assessment of performance

The results obtained by applying the three snow schemes are in agreement with previous findings, suggesting that the complexity of the representation of snow within LPJ-GUESS has a significant influence on both simulated snow and soil properties.

The major disagreement between the *Static* simulation and observed temperatures in Figure 3.4 for the set of Russian sites suggests that this scheme could, potentially, only yield realistic results if the constant parameters are optimised for the chosen study region. This is supported by the relatively good performance of the optimised *Static* set-up for the Sodankylä site. The *Simple multi-layer* scheme performed better at broad scales - predicting the insulation capacity for the set of Russian sites - than in the single-site analysis. Based on the outcomes of this study, it appears that the new intermediate complexity snow scheme (*Advanced multi-layer* scheme) has the skill to adequately simulate snow dynamics both at the local and regional scale. The computed R^2 and RMSE values suggest that this new dynamic snow scheme is able to simulate snow micro-structure, layer distribution and density variability more realistically than the other schemes. Snow density is a key variable, since the variables regulating insulation capacity (thermal properties, conductivity and heat capacity) are derived from it. Hence, it is a link between above- and sub-surface conditions. Simulating density mechanistically is an important step to assess complex snow-soil relationships in the future. The misfit compared to measurements, however, suggests that further improvements in the scheme could enhance the model's performance.

This section has reviewed the key aspects of the results, the behaviour of each scheme is discussed in detail in the following sections, according to the project's structure.

4.2 Sodankylä site simulations

The single-site analysis sought to investigate how the optimised models' performance differs using the three applied snow schemes, while validating results with observational station data.

In Figure 3.2 we can see that the *Static* scheme with constant snow density and thermal conductivity can reproduce the snowfall patterns at the Finnish site. Rautiainen et al. (2014) stated that the average annual snow density is 170-200 kg m⁻³, which explains why the customised *Static* scheme with a constant 200 kg m⁻³ snow density corresponds well to the measured snow height. Using observed precipitation as model input data also increased the fit between simulated and measured snow depths. As pointed out in the Results section, the *Simple multi-layer* scheme captures the snow height, although Figure 3.2 b shows that there is a broad spread of simulated snow depths. This finding suggests that, in general terms, the *Static* scheme performs better than the *Simple multi-layer* one. The *Simple multi-layer* scheme is unable to capture the snow dynamics at this site, which in turn affects the sub-surface thermal regime. Even though the *Advanced multi-layer* scheme is more complex, the fit between observed and modelled snow depth and soil temperature entities are comparable - after customising the snow temperature threshold and density range parameters to match local conditions. The design of the integrated compaction scheme could be the reason why the *Advanced multi-layer* scheme is consistently underestimates snow height at Sodankylä. The compaction rate was significantly lowered for these simulations, yet the resulting layer densities prove to be higher than the observations. Another reason behind this misfit could be that compaction occurs continuously for each day that at least one snow layer exists. In reality, compaction is dependent on several factors, e.g. wind

forcing, grain size, temperature gradient within the snow pack and liquid water content among others. Aiming at the simplest structural representation, these processes are not taken into account in this study, but will be addressed in the future.

Regarding the soil thermal regime, an interesting feature in Figure 3.3 is that the *Static* scheme consistently underestimates soil temperature during the winter period. The modelled snow depth values are higher than measured, which suggests a higher insulation capacity and thus higher than measured soil temperatures - as observed for the *Simple multi-layer* set-up. The deviations between simulated and measured soil temperatures during the winter period, using the *Advanced multi-layer* set-up, can be attributed to the thinner simulated snow pack, shown in Figure 3.2 a. Denser snow layers build up a thinner snow pack, with a lower insulation capacity, which could contribute to the underestimation of soil temperatures. The computed soil temperatures are also influenced by the structural representation of snow layers, which can be observed in the temperature profile sketch in Figure 1.2. In case the layers have the same density and thermal properties (*Simple multi-layer* scheme), the change in temperature from the atmosphere towards the soil surface would be abrupt, without a gradient in the snow pack (blue dashed line). On the other hand, accounting for the layer's specific density and conductivity (*Advanced multi-layer* scheme) makes it possible to simulate a step-wise change in temperature within the snow pack (minimum curve). This calculation method suggests that applying the *Simple multi-layer* set up the temperature difference between atmosphere and soil would be bigger, and the calculated soil temperatures therefore higher than with the *Advanced multi-layer* scheme with individual snow layers. Differences during the summer peak period for all three schemes may be caused by soil upper layer moisture content, which affects soil thermal conductivity. Phase changes and internal, sub-daily transport of water between snow layers towards the soil are not simulated, even though these features could affect soil hydrological conditions. After implementing a more realistic melt-water treatment and frozen-liquid water fractionation, this feature can be re-evaluated, and potentially corrected.

Thus far, we evaluated the potential for small scale application and argued that the newly developed *Advanced multi-layer* scheme is suitable for further analysis. The section that follows moves on to assess the snow insulation effect at a regional scale, while applying the different set-ups.

4.3 Evaluation of air-soil temperature differences

The main objective of this section is to compare the performance of the three snow schemes to the findings of Wang et al. (2016).

Air-soil temperature

Regarding the insulation effect (ΔT), the *Simple multi-layer* scheme results resemble the most the observational pattern, although it overestimates ΔT for snow depths from 40-50 cm and higher. The Sodankylä site runs (Figure 3.3) also showed that the *Simple multi-layer* scheme simulates higher than measured soil temperatures along the soil profile. Applying the *Advanced multi-layer* scheme, the model is able to capture the differences between the three temperature regimes, where the air-soil temperature difference is the highest for the group with an air temperature of -25 °C or colder. Wang et al. (2016) point out that the snow insulation effect is expected to be lower in case the model is underestimating snow height, because thick snow insulates better than thin snow. This feature can be seen in Figure 3.4 a, where the magnitude of insulation is significantly lower for the *Advanced multi-layer* scheme compared to the observations.

The insulation saturation effect can be noted in the observation and *Simple multi-layer* scheme plots in Figure 3.4. It appears that increases in already thick snow influences soil temperature less, since the curves level off at a height of approximately 40 cm. This feature is consistent with

the findings of Slater, Lawrence, and Koven (2017), although they suggest that the snow insulation effect drops above approximately 25 cm. The *Advanced multi-layer* scheme has a lower amplitude for ΔT , and the threshold effective snow depth is barely visible. The lower than observed insulation capacity along all snow depth classes indicates that the calculated snow thermal conductivity is probably higher than in reality. This results in a lower air-soil temperature difference due to a weaker insulation.

Soil temperature

Looking at soil temperature variations, the *Static* scheme performs poorly, which could be expected from the corresponding graph in Figure 3.4 a. Minor developments on the model since the publication by Wang et al. (2016), along with the different meteorological forcing data might be the reasons why the *Static* scheme provides significantly different results than the ones reported by Wang et al. (2016). This is discussed in the next paragraph. Just as for ΔT , the *Simple multi-layer* scheme set up resembles the observational pattern the most. The decrease in soil T with increasing snow height is, however, steeper than the measured rate. The *Advanced multi-layer* scheme captures the soil temperature-snow height relationship between different temperature regimes, but shows a negative shift by approximately 5 °C compared to the reference plot. Although the *Advanced multi-layer* scheme is the most complex out of the three tested schemes, there are still important processes missing from the framework, as mentioned in the previous paragraph. Pomeroy and Brun (2001) state that the presence and quantity of liquid water within a snow layer can influence the compaction rate by changing the snow's viscosity factor. Including ice-liquid water fractionation may affect the simulated insulation behaviour.

As indicated previously, the *Static* scheme performed poorly both in regard to ΔT and soil temperature relationships. The insulation effect observed for this scheme was well below the reported results of Wang et al. (2016). Given the different climatic forcing dataset and the computed bias compared to measured air temperature, we decided to test how warmer conditions would influence the insulation capacity for the *Static* and *Advanced multi-layer* schemes. We saw no effect on the performance for the *Static* set-up.

Increasing the air temperature by 4.7 °C - the reported bias for CRU NCEP4 dataset (Viovy and Ciais, 2011) - resulted in a stronger insulation effect for the *Advanced multi-layer* scheme. What stands out on Figure A.2 is that, while the soil temperature curve follows a similar asymptotic trend as the observations, the warmest temperature class behaves much like the default simulations. The air temperature bias computed for the CRU NCEP version 7 dataset used for our simulations is -0.4 °C - significantly lower than for the earlier dataset. The 1.4 °C RMSE (root mean squared error) suggests that the applied version is suitable for the regional analysis and that the results presented in Figure 3.4 are valid. The higher air temperature test nevertheless showed that the accuracy of air temperature forcing data can considerably influence small scale simulations. Even though the increased air temperature test resulted in a higher insulation effect for the *Advanced multi-layer* scheme (seen in Figure A.2, left column), the findings of the bias analysis suggest that the model-observation deviations are caused primarily by structural differences in the schemes, and not by the different climatic forcing data.

4.4 Evaluation of permafrost dynamics

Surface conditions, such as snow cover and snow height, directly influence sub-surface conditions at high latitudes. During the winter period, snow dampens the air's cooling effect, resulting in higher near surface soil temperatures which affect the rate and depth of thawing. We expected that the structural differences would significantly influence simulated permafrost properties, since the previous sections showed that the representation of snow related processes has an effect on both simulated snow dynamics and soil temperatures.

ALD trends at CALM sites (1996-2000)

Figure 3.5 and Table 3.3 confirm this hypothesis, showing the differences between the used schemes' performance. As mentioned in the Results section, the average observed and modelled ALD between 1996-2015 does not align well at the selected sites. The time series analysis (Figure 3.6) shows that at sites U19, S2, R2 and C7A the simulated ALD reaches the predefined maximum of 150 cm. At other locations - U6, S2, R19, R5, C7A - the *Advanced multi-layer* scheme is able to capture the inter-annual variability, even though there's an offset in the active layer depth. Luo et al. (2016) studied the spatio-temporal variations in active layer thickness based on observations at several CALM sites, including the ones chosen for this project. They found a significant trend in ALD at 6 out of our 10 sites - U6, U19, G2, S2, R19, R2. These sites are marked with a star on Figure 3.6. From these marked sites, LPJ-GUESS can simulate similar trends at sites S2, R19, U6 and G2.

Quantitatively comparing observed and modelled ALD is a challenging task. The observational scale and the model's spatial resolution do not correspond, and with the use of global gridded climatic forcing and other global forcing datasets the site specific characteristics that may influence permafrost properties cannot be replicated. Given that LPJ-GUESS is customised to regional and not local applications, the misfit at the selected CALM sites does not necessarily mean that the model performs poorly in terms of permafrost related entities. The Sodankylä site analysis confirmed that using site specific meteorological data and optimising snow parameters to capture the site characteristics improved the fit between observed and modelled snow depth and soil temperature. Accounting for soil types, soil organic material content, and possibly peat at the sites would also increase the accuracy of simulated permafrost-related entities.

Spatial analysis

Spatial patterns of permafrost cover were investigated to get a fuller picture of how accurate the ALD simulations are at a broad scale. In Figure 3.6 we can observe the pattern seen at the Sodankylä site earlier: the *Simple multi-layer* scheme simulates warmer winter-time soil temperatures than the other two schemes, and consequently estimates a smaller permafrost covered area. The other schemes simulate the lowest ALD in Northern-Central Siberia, where the coldest wintertime soil temperatures are noted. The model's estimated permafrost underlain area with the *Static* and *Advanced multi-layer* schemes is comparable to estimations seen in Figure 1.1 by Brown et al. (2002) and reported by Koven, Riley, and Stern (2013) and McGuire et al. (2018).

Even though this sub-project provided a qualitative interpretation and comparison of the three schemes' performance, we can conclude that the differences observed at the local and multi-site analysis are visible on the Arctic scale as well. These results suggests that further investigation is needed to quantify these deviations and provide a quantitative assessment of permafrost conditions - including ALD, permafrost extent, soil carbon stock estimates - using the three applied snow schemes. Advances in this direction can enable to assess the importance of snow for the soil thermal dynamics on the Pan-Arctic region.

Adequately simulating snow-soil interactions and soil thermal dynamics is key in estimating changes in active layer thickness, which can be used as a proxy for the degree and rate of permafrost degradation through time and space.

4.5 Shortcomings and future improvements

The main goal of this study was to test and compare the different complexity snow schemes in LPJ-GUESS and assess their influence on derived model outputs. For this reason, the model was used in a default set up, not including a litter or moss cover on the soil surface, nor with Arctic-specific PFTs (plant functional types). These factors could be important to account for when the aim is to evaluate global greenhouse gas fluxes. Wind is not included in LPJ-GUESS, which would be an important agent in defining snow microtopography, redistributing freshly fallen snow and affecting density by creating high density wind-slab layers. Horizontal processes and shading effects by vegetation are not accounted for. Due to the hard snow temperature threshold, rain and snow cannot coexist in the simulations. The effect of this, however, on the evaluated output entities is probably marginal.

Even though the new *Advanced multi-layer* scheme presented here is the most complex of the three tested frameworks in this project, there is room for potential structural improvements within the scheme. A recent model evaluation study (Slater, Lawrence, and Koven, 2017) highlighted that there are several potential biases in evaluating modelled soil temperatures. The results could be considerably different if the models include a highly insulating organic layer, information about soil texture, thickness and number of soil layers and water phases within the snow pack. Regarding the *Advanced multi-layer* scheme, the snow pack's internal topography may be further refined. Enabling ice and liquid water differentiation within layers would be an important process to take into account regarding the storage and refreezing of liquid water (Esery et al., 2013). Simulations of phase changes and the transport of melt water between layers, and finally to the soil, can connect the updated scheme with the hydrology module. Changes in soil moisture in relation to snow cover changes can be analysed after applying these refinements. Collectively, these alterations can further improve the performance of LPJ-GUESS in relation to wintertime processes.

5 Conclusion

The purpose of this project was to examine the snow insulation capacity in LPJ-GUESS, while applying three different complexity snow schemes. The study found that the representation of snow within the model has a significant effect on the soil thermal regime, and directly on the derived permafrost-related properties. The findings of this study complement those of earlier studies, suggesting that snow cover is a key factor in determining soil thermal dynamics.

Confirming our hypothesis, the project showed that LPJ-GUESS has the skill to adequately simulate snow dynamics at a local scale, when forced with site meteorological data. The regional analysis highlighted that the *Advanced multi-layer* scheme produces a lower insulation effect than suggested by observations, although it is able to capture the observed soil-air temperature and snow depth relationship. The *Simple multi-layer scheme* performed best at capturing the snow insulation effect at the Russian sites, but the single-site and Pan-Arctic analyses highlighted that the simulated soil temperatures are significantly higher than observed for this model set-up. We also identified that some key processes are currently missing from the intermediate complexity framework.

Developing the structural representation in the model enables an assessment of regional snow-soil-vegetation interactions. This could help to evaluate how carbon-rich permafrost soils will behave at high latitudes under future climate scenarios. Permafrost degradation, which can lead to increased greenhouse gas emissions, and vegetation composition shifts are some of the most significant projected changes that will be investigated in future projects.

Notwithstanding some limitations, the results suggest that with an intermediate complexity snow scheme LPJ-GUESS can achieve a more realistic simulation of wintertime processes. Further research will explore the implications of these changes in relation to global greenhouse gas cycles and spatio-temporal patterns.

A Supplementary data

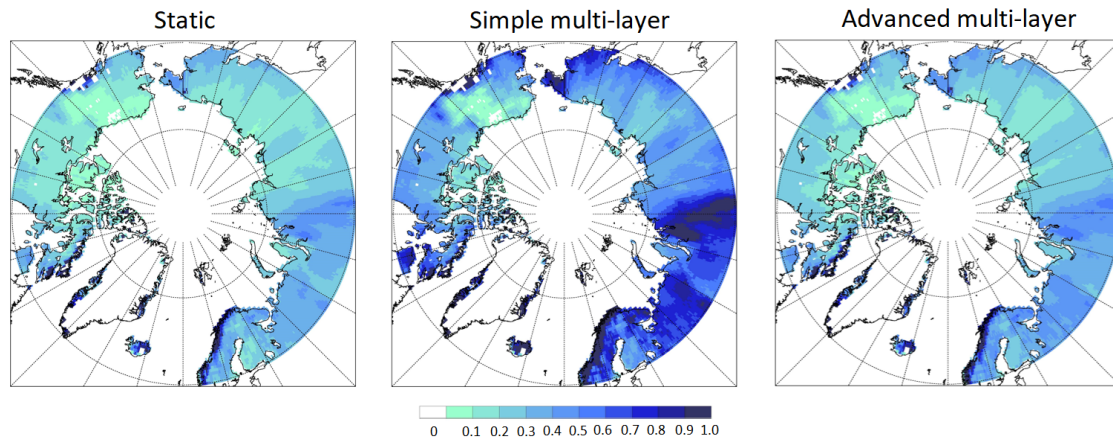


FIGURE A.1: Average spatial snow depth patterns between 1996 and 2000, applying the *Static*, *Simple*- and *Advanced-multi-layer* schemes, respectively.

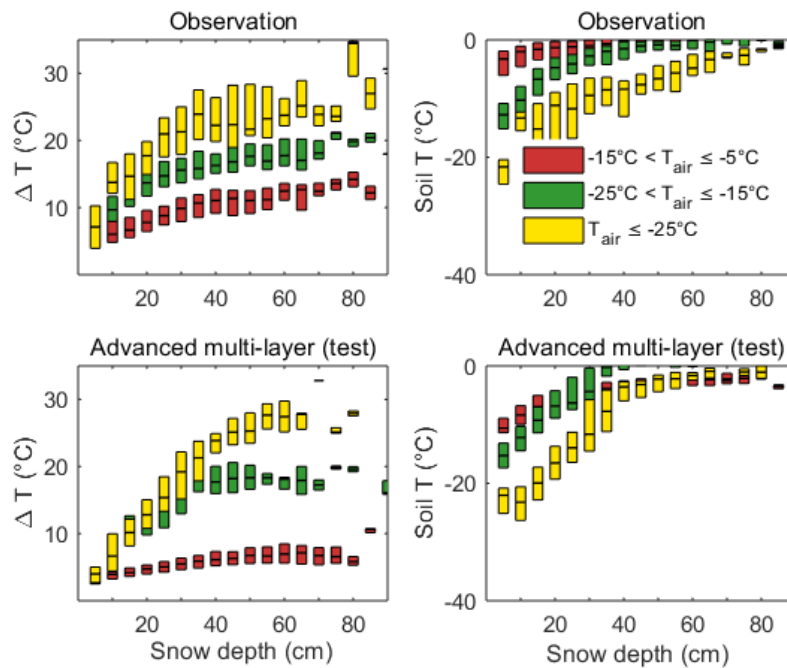


FIGURE A.2: Sensitivity-like test results at the Russian study sites (*Advanced multi-layer* scheme), increasing air temperature by 4.7°C . a) ΔT and snow depth relationship. b) Soil T at 25 cm depth and snow depth relationship.

TABLE A.1: R^2 and root mean squared error (RMSE) between observed and modelled snow depth at Sodankylä, 2007-2014 for each tested schemes.

	R^2	RMSE (cm)
Static	0.84	12.41
Simple multi-layer	0.71	15.45
Advanced multi-layer	0.88	10.7

TABLE A.2: Selected CALM sites for the ALD trend analysis.

Site name	Site code	Location (lat/lon)
Barrow	U2	71.32°N, 156.6°W
Deadhorse	U6	70.17°N, 148.47°W
Pearl Creek	U19	64.9°N, 147.8°W
Zackenberg, ZEROCALM 2	G2	74.46°N, 20.56°W
Abisko area, Sweden	S2	68.33°N, 18.84°W
Ayach-Yakha, Vorkuta	R2	67.58°N, 64.18°E
Vaskiny Dachy, Yamal Peninsula	R5	70.28°N, 68.9° E
Lake Glukhoe, Kolyma	R19	68.8°N, 160.95°E
Bykovsky (Lena delta)	R29A	71.78°N, 129.42°E
Reindeer Depot	C7A	68.68°N, 134.13° W

List of Figures

1.1	The Pan-Arctic study region and estimated permafrost cover by the Circumpolar Active Layer Monitoring program (Brown et al., 2002). Retrieved from http://www.grida.no/resources/5234 ; Accessed 3 January, 2019; Credit: Hugo Ahlenius UNEP/GRID-Arendal.	1
1.2	Theoretical subsurface temperature profile (Koven, Riley, and Stern, 2013). Potential snow cover - shown by the shaded grey area - effectively dampens the cooling effect of air during the cold season. The dashed line shows the average temperature profile; solid lines the seasonal maximum and minimum annual curves.	3
2.1	Snow pack design of the <i>Advanced multi-layer</i> scheme (C1-C5 denotes the compaction in each layer).	10
2.2	Work-flow of the updates in the <i>Advanced multi-layer</i> scheme.	11
3.1	Average snow layer properties in Sodankylä, applying the <i>Advanced multi-layer</i> snow scheme. Colours denote the different snow layers. a) Snow layer division and layer snow water equivalent (SWE) averages per month. b) Simulated snow pack structure at Sodankylä, during a selected snow season.	13
3.2	a) Observed and simulated snow depth at Sodankylä, 2007/11 to 2014/7. Continuous lines represent different model set-ups, the dashed line observed snow height. b) Observed and measured snow depth relationship at Sodankylä (2007-2014). Colours represent different model set-ups.	14
3.3	Observed and modelled soil temperature at six depths, between 2011/11 and 2014/7.	14
3.4	Snow insulation effect 1980-2000, DJF, observations and model simulations using three snow schemes. Snow depth presented on the horizontal axis is classified in 5 cm depth bins. Colours indicate different air temperature regimes. Upper and lower bars present the 25th and 75th percentiles. a). Difference in air-soil temperature and snow depth relationship. b). Soil temperature and snow depth relationship.	16
3.5	Maximum seasonal ALD for 10 CALM sites, observations and model simulations, applying three different snow schemes. Sites with a * are marked by Luo et al. (2016) having significant observational trends in ALD.	18
3.6	Pan-Arctic simulations applying the three tested snow schemes, average 1996-2015. Top row: Maximum ALD (in meters), Bottom row: Average winter (DJF) soil temperature at 25 cm depth (in °C).	19
A.1	Average spatial snow depth patterns between 1996 and 2000, applying the <i>Static</i> , <i>Simple</i> - and <i>Advanced-multi-layer</i> schemes, respectively.	26
A.2	Sensitivity-like test results at the Russian study sites (<i>Advanced multi-layer</i> scheme), increasing air temperature by 4.7 °C. a) Delta T and snow depth relationship. b) Soil T at 25 cm depth and snow depth relationship.	26

List of Tables

1.1	Approximate ranges for key snow variables retrieved from literature sources.	2
2.1	Input and evaluation data used for this project. Observations are retrieved from: ¹ FMI, ² Russian Research Institute of Hydrometeorological Information: World Data Centre, ³ CALM Summary Data Table	7
2.2	Description of key snow variables.	8
2.3	Characteristics of the applied schemes. ¹ Wania, Ross, and Prentice (2009), ² Best et al. (2011), ³ Ling and Zhang (2006)	11
3.1	Soil temperature R^2 for the three snow schemes at Sodankylä (2011-2014).	15
3.2	Soil temperature RMSE (°C) for the three snow schemes at Sodankylä (2011-2014) .	15
3.3	Average annual maximum ALD of selected CALM sites (1996-2015).	17
A.1	R^2 and root mean squared error (RMSE) between observed and modelled snow depth at Sodankylä, 2007-2014 for each tested schemes.	27
A.2	Selected CALM sites for the ALD trend analysis.	27

Bibliography

- Best, M. J. et al. (2011). “The Joint UK Land Environment Simulator (JULES), model description “ Part 1: Energy and water fluxes”. In: *Geoscientific Model Development* 4.3, pp. 677–699. DOI: [10.5194/gmd-4-677-2011](https://doi.org/10.5194/gmd-4-677-2011).
- Brown, J. et al. (2002). “Circum-Arctic Map of Permafrost and Ground-Ice Conditions, Version 2”. In:
- Choudhury, Bhaskar J. and Nicolo E. DiGirolamo (1998). “A biophysical process-based estimate of global land surface evaporation using satellite and ancillary data I. Model description and comparison with observations”. In: *Journal of Hydrology* 205.3, pp. 164–185. ISSN: 0022-1694. DOI: [https://doi.org/10.1016/S0022-1694\(97\)00147-9](https://doi.org/10.1016/S0022-1694(97)00147-9).
- Christensen, Torben R et al. (2017). “Arctic carbon cycling”. English. In: *Snow, Water, Ice and Permafrost in the Arctic (SWIPA) 2017*. Ed. by AMAP. AMAP (Arctic Monitoring and Assessment Programme), pp. 203–218. ISBN: ISBN 978-82-7971-101-8.
- Essery, R. et al. (2016). “A 7-year dataset for driving and evaluating snow models at an Arctic site (Sodankylä, Finland)”. In: *Geoscientific Instrumentation, Methods and Data Systems* 5.1, pp. 219–227. DOI: [10.5194/gi-5-219-2016](https://doi.org/10.5194/gi-5-219-2016).
- Essery, Richard et al. (2013). “A comparison of 1701 snow models using observations from an alpine site”. In: *Advances in Water Resources* 55. Snow–Atmosphere Interactions and Hydrological Consequences, pp. 131–148. ISSN: 0309-1708. DOI: <https://doi.org/10.1016/j.advwatres.2012.07.013>.
- Gerten, Dieter et al. (2004). “Terrestrial vegetation and water balance—hydrological evaluation of a dynamic global vegetation model”. In: *Journal of Hydrology* 286.1, pp. 249–270. ISSN: 0022-1694. DOI: <https://doi.org/10.1016/j.jhydrol.2003.09.029>.
- Gouttevin, I. et al. (2012). “How the insulating properties of snow affect soil carbon distribution in the continental pan-Arctic area”. In: *Journal of Geophysical Research: Biogeosciences* 117.G2. DOI: [10.1029/2011JG001916](https://doi.org/10.1029/2011JG001916).
- Harris, Ian et al. (2014). “Updated high-resolution grids of monthly climatic observations—The CRU TS3.10 Dataset”. In: *International Journal of Climatology* 34, n/a–n/a. DOI: [10.1002/joc.3711](https://doi.org/10.1002/joc.3711).
- Keenan, Trevor and William Riley (2018). “Greening of the land surface in the world’s cold regions consistent with recent warming”. In: *Nature Climate Change* 8. DOI: [10.1038/s41558-018-0258-y](https://doi.org/10.1038/s41558-018-0258-y).
- Koven, Charles, William Riley, and Alex Stern (2013). “Analysis of Permafrost Thermal Dynamics and Response to Climate Change in the CMIP5 Earth System Models”. In: *Journal of Climate* 26, pp. 1877–1900. DOI: [10.1175/JCLI-D-12-00228.1](https://doi.org/10.1175/JCLI-D-12-00228.1).
- Krinner, Gerhard et al. (2018). “ESM-SnowMIP: Assessing models and quantifying snow-related climate feedbacks”. In: *Geoscientific Model Development Discussions*, pp. 1–32. DOI: [10.5194/gmd-2018-153](https://doi.org/10.5194/gmd-2018-153).
- Lawrence, David M. and Andrew G. Slater (2010). “The contribution of snow condition trends to future ground climate.” In: *Climate Dynamics* 34.7/8, pp. 969–981. ISSN: 09307575.
- Le Quéré, C. et al. (2018). “Global Carbon Budget 2017”. In: *Earth System Science Data* 10.1, pp. 405–448. DOI: [10.5194/essd-10-405-2018](https://doi.org/10.5194/essd-10-405-2018).
- Leppänen, L. et al. (2016). “Sodankylä manual snow survey program”. In: *Geoscientific Instrumentation, Methods and Data Systems* 5.1, pp. 163–179. DOI: [10.5194/gi-5-163-2016](https://doi.org/10.5194/gi-5-163-2016).
- Ling, Feng and Tingjun Zhang (2006). “Sensitivity of ground thermal regime and surface energy fluxes to tundra snow density in northern Alaska”. In: *Cold Regions Science and Technology* 44, pp. 121–130. DOI: [10.1016/j.coldregions.2005.09.002](https://doi.org/10.1016/j.coldregions.2005.09.002).

- Luo, Dongliang et al. (2016). "Recent changes in the active layer thickness across the northern hemisphere". In: *Environmental Earth Sciences* 75.7, p. 555. ISSN: 1866-6299. DOI: [10.1007/s12665-015-5229-2](https://doi.org/10.1007/s12665-015-5229-2).
- Luojus, K. et al. (2011). "Investigating hemispherical trends in snow accumulation using Glob-Snow snow water equivalent data". In: pp. 3772–3774. ISSN: 2153-7003. DOI: [10.1109/IGARSS.2011.6050051](https://doi.org/10.1109/IGARSS.2011.6050051).
- Mackiewicz, Michael C. (2012). "A new approach to quantifying soil temperature responses to changing air temperature and snow cover". In: *Polar Science* 6.3, pp. 226–236. ISSN: 1873-9652. DOI: <https://doi.org/10.1016/j.polar.2012.06.003>.
- McGuire, A. David et al. (2018). "Dependence of the evolution of carbon dynamics in the northern permafrost region on the trajectory of climate change". In: *Proceedings of the National Academy of Sciences*. ISSN: 0027-8424. DOI: [10.1073/pnas.1719903115](https://doi.org/10.1073/pnas.1719903115).
- McGuire A.D. and Christensen, T.R. et al. (2012). "An assessment of the carbon balance of Arctic tundra: Comparisons among observations, process models, and atmospheric inversions." In: *Biogeosciences* 9.8, pp. 3185–3204. ISSN: 17264170.
- Meyer, Leo et al. (2014). *IPCC, 2014: Climate Change 2014: Synthesis Report. Contribution of Working Groups I, II and III to the Fifth Assessment Report of the Intergovernmental Panel on Climate Change*. Tech. rep. Geneva, Switzerland, pp. 3–87.
- Oleson, Keith, David Lawrence, and G.B. Bonan (2013). "Technical description of version 4.5 of the Community Land Model (CLM). Ncar Tech. Note NCAR/TN-503+STR. National Center for Atmospheric Research, Boulder". In:
- Peng, S. et al. (2016). "Simulated high-latitude soil thermal dynamics during the past 4 decades". In: *The Cryosphere* 10.1, pp. 179–192. DOI: [10.5194/tc-10-179-2016](https://doi.org/10.5194/tc-10-179-2016).
- Peters, Wouter et al. (2018). "Increased water-use efficiency and reduced CO₂ uptake by plants during droughts at a continental scale". In: *Nature Geoscience* 11. DOI: [10.1038/s41561-018-0212-7](https://doi.org/10.1038/s41561-018-0212-7).
- Pomeroy, J. W. and E. Brun (2001). *Physical Properties of Snow*.
- Rautiainen, Kimmo et al. (2014). "Detection of soil freezing from L-band passive microwave observations". In: *Remote Sensing of Environment* 147, pp. 206–218. ISSN: 0034-4257. DOI: <https://doi.org/10.1016/j.rse.2014.03.007>.
- Slater, A. G., D. M. Lawrence, and C. D. Koven (2017). "Process-level model evaluation: a snow and heat transfer metric". In: *The Cryosphere* 11.2, pp. 989–996. DOI: [10.5194/tc-11-989-2017](https://doi.org/10.5194/tc-11-989-2017). URL: <https://www.the-cryosphere.net/11/989/2017/>.
- Slater, Andrew G. and David M. Lawrence (2013). "Diagnosing Present and Future Permafrost from Climate Models". In: *Journal of Climate* 26.15, pp. 5608–5623. DOI: [10.1175/JCLI-D-12-00341.1](https://doi.org/10.1175/JCLI-D-12-00341.1).
- Smith, B. et al. (2014). "Implications of incorporating N cycling and N limitations on primary production in an individual-based dynamic vegetation model". In: *Biogeosciences* 11.7, pp. 2027–2054. DOI: [10.5194/bg-11-2027-2014](https://doi.org/10.5194/bg-11-2027-2014).
- Smith, Benjamin, I. Colin Prentice, and Martin T. Sykes (2001). "Representation of vegetation dynamics in the modelling of terrestrial ecosystems: comparing two contrasting approaches within European climate space". In: *Global Ecology and Biogeography* 10.6, pp. 621–637. DOI: [10.1046/j.1466-822X.2001.t01-1-00256.x](https://doi.org/10.1046/j.1466-822X.2001.t01-1-00256.x).
- Sturm, Matthew et al. (1997). "The thermal conductivity of seasonal snow". In: *Journal of Glaciology* 43.143, 26–41. DOI: [10.3189/S0022143000002781](https://doi.org/10.3189/S0022143000002781).
- Viovy, Nicolas (2016). "CRUNCEP Version 7 - Atmospheric Forcing Data for the Community Land Model". In: URL: <http://rda.ucar.edu/datasets/ds314.3/>.
- Viovy, Nicolas and Philippe Ciais (2011). "CRUNCEP data set for 1901–2008, Tech. Rep. Version 4". In: *Laboratoire des Sciences du Climat et de l'Environnement*.

- Wang, Wenli et al. (2016). "Evaluation of air-soil temperature relationships simulated by land surface models during winter across the permafrost region". English. In: *Cryosphere* 10.4, pp. 1721–1737. ISSN: 1994-0416. DOI: [10.5194/tc-10-1721-2016](https://doi.org/10.5194/tc-10-1721-2016).
- Wania, R., I. Ross, and I. C. Prentice (2009). "Integrating peatlands and permafrost into a dynamic global vegetation model: 2. Evaluation and sensitivity of vegetation and carbon cycle processes". In: *Global Biogeochemical Cycles* 23.3. DOI: [10.1029/2008GB003413](https://doi.org/10.1029/2008GB003413).
- Zaehle, Sönke et al. (2014). "Evaluation of 11 terrestrial carbon–nitrogen cycle models against observations from two temperate Free-Air CO₂ Enrichment studies". In: *New Phytologist* 202.3, pp. 803–822. ISSN: 1469-8137. DOI: [10.1111/nph.12697](https://doi.org/10.1111/nph.12697).
- Zhang, Wenxin et al. (2014). "Biogeophysical feedbacks enhance the Arctic terrestrial carbon sink in regional Earth system dynamics". English. In: *Biogeosciences* 11.19, pp. 5503–5519. ISSN: 1726-4170. DOI: [10.5194/bg-11-5503-2014](https://doi.org/10.5194/bg-11-5503-2014).